Research Article

# Investigation of the source, morphology, and trace elements associated with atmospheric $PM_{10}$ and human health risks due to inhalation of carcinogenic elements at Dehradun, an Indo-Himalayan city

Vignesh Prabhu[1] · Vijay Shridhar[1] · Arti Choudhary[2]

## Abstract

To study the physical and chemical properties of atmospheric particulate matter over Dehradun city located along the foothills of the Himalayas, both in situ and satellite-based observations were utilized in the present research. Ambient respirable suspended particles denoted by $PM_{10}$ (atmospheric particulate matter having an aerodynamic diameter of ≤ 10 μm) was measured during 2016–2017. The morphology and elemental characteristics of $PM_{10}$ was studied through scanning electron microscopy (SEM) and SEM-energy-dispersive X-ray spectroscopy, respectively. The 24-h mean ± standard deviation of $PM_{10}$ was observed to be 158.6 ± 33.4 μg/m$^3$, which is more than 2 times the permissible limit of World Health Organization (50 μg/m$^3$). Microscopic analysis revealed particles with irregular, porous, rounded, flaky, chain and branched structures indicating various types such as tar balls, soot, crystalline and biogenic particles. The frequently found particle types were investigated for the atomic percentage contribution, which revealed vehicular exhaust, industrial emission, biomass burning, and crustal/dust re-suspension as the chief source of $PM_{10}$. To delineate the source and transport pathway of air masses converging over the city, 24-h air mass back trajectories were associated with MODerate resolution Imaging Spectroradiometer derived fire spots, geographical location of cement manufacturing and thermal power plants in the vicinity of monitoring site. Excess cancer risk due to inhalation of Lead particles (mean = 0.159 μg/m$^3$) associated with $PM_{10}$ was $0.16 \times 10^{-6}$, which is well below the safe limit ($1 \times 10^{-6}$) framed by the United States Environment Protection Agency.

Keywords  Aerosols · Scanning electron microscope · Morphology · Back trajectory · Excess cancer risk

## 1 Introduction

The swift pace of urbanization and industrialization has contributed substantially toward the elevation of air pollution levels, especially in the developing countries. Atmospheric particulate matter (PM) considered as one of the criteria air pollutants [1] is diverse and complex to understand in terms of source, morphology, composition, size distribution, and mixing state [2]. In India, most of the research studies on atmospheric PM have focused on the elemental composition of particles [3–5]. However, several researchers have investigated both the physical (shape and size) and elemental characteristics of atmospheric PM through scanning electron microscope (SEM) and

SEM-energy-dispersive X-ray spectroscopy (SEM–EDX), respectively [6–8]. At the coastal city of Chennai, located in the south of India, SEM analysis revealed particle types such as soot, minerals and salts, whose origination can be traced to combustion, crustal and marine sources, respectively [9, 10]. In a densely populated city of Agra, located in the Indo-Gangetic Plains (IGP), SEM analysis revealed alumino-silicates, soot and tarball-type particles indicating contribution from construction, coal burning, and crustal sources [11]. Similarly, at the metropolitan city of New Delhi, located in IGP, SEM analysis revealed crystalline, soot and flaky type particles indicating substantial contribution from vehicular, crustal and long-range sources [12]. However, information on particulate morphology in the Himalayan region is scarce.

Besides, morphological profile of atmospheric particles, information of chemical species associated with the particles can act as markers to identify the emission sources. For example, some common markers for vehicular emission includes copper (brake lining), zinc (tire wear), aluminum (wear of piston), iron (wear and tear of brake) and manganese (additives in unleaded gasoline) [13]. Crustal/soil dust emissions are identified by tracer elements such as calcium, iron, magnesium, silica, manganese, potassium, sodium, lead, zinc, and copper [14]. However, the elements emitted from industrial chimneys depend on the type of manufacturing processes.

Over the last few years, numerous epidemiological studies have been conducted worldwide on finding the association between air pollution and human mortality [15]. These findings reveal the importance of monitoring atmospheric $PM_{10}$ especially in the data deficit regions. Moreover, it is well known that the exposure of carcinogenic heavy metals associated with $PM_{10}$ can strongly induce carcinogenicity in humans [16]. However, information of the atmospheric PM-associated elemental composition is scarcely available over complex terrains. Therefore, this research work was framed to fill a substantial part of this knowledge gap, thereby aiding in understanding the aerosol dynamics over urban-cities situated in valley-based complex topography. The objectives of this present study were to estimate the mass concentration of $PM_{10}$, along with its morphology, source and health risks of atmospheric $PM_{10}$.

## 2 Materials and methods

### 2.1 Details of the study site

The atmospheric $PM_{10}$ measurement was carried out at Dehradun city (30.28°N latitude and 77.99°E longitude) geographically located between the lower and Siwalik Hills

(Fig. S1 of supplementary text). The city is situated at an altitude of 640 m above mean sea level with a total area of 300 km$^2$ (https://dehradun.nic.in). Dehradun district has a population density of 549 persons/km$^2$, and over the past decade (2001–2011), the population has increased by 32% along with a burgeoned increase in about 34 times in the total number of registered vehicles in Uttarakhand state (http://ueppcb.uk.gov.in/). The city is surrounded by dense forest comprising chiefly of Sal tree (*Shorea robusta*), and the climate is generally temperate. The city offers a lot of growth opportunities for people from surrounding mountainous regions [17]. In order to accommodate the large inflow of migrants, the city has been undergoing a rapid expansion in urban spaces. Dehradun city was placed at thirty-first position in the list of top 100 polluting cities in the world [18].

### 2.2 Atmospheric $PM_{10}$, meteorological and vehicular data collection

For measuring the atmospheric $PM_{10}$, respirable dust sampler (Model No: SLE-RDS104NL, Spectro Lab, India) was operated at a flow rate of 1.1 m$^3$/min controlled by a flow meter. The sampler inlet was placed at 3 m above ground level (AGL) to avoid any obstruction in air flow. Sampling was performed during the winter (November, December in the year 2016 and January of 2017) and summer season (March, April, and May of 2017). A total of 160 samples were collected with 80 samples from each season. The duration of sampling was 24 h, i.e., 6 AM on the first day to 6 AM on the next day (IST, Indian Standard Time). The EPM2000 grade glass fiber filter paper was desiccated for 24 h before and after sampling and weighted using an electronic balance (Model No: XS105DU, Mettler Toledo, USA). As a quality assurance and quality control measure, the filter papers were handled using forceps, transported in a sealed box and maintained in dust free condition during sampling and analysis [19]. Moreover, a blank filter paper was collected every month during sampling period and the final results are blank corrected.

During winter and summer season, the average temperature, relative humidity, visibility, and wind speed was observed to be 16.39 °C, 73.53%, 2.23 km, 1.96 km/hr and 24.60 °C, 49.33%, 2.79 km, 2.83 km/hr, respectively. The 24-h average values of meteorological parameters were acquired from weather underground (https://www.wunderground.com), and the results are furnished in Fig. S2 of supplementary text.

The vehicular count was performed twice in week (once each during weekday and weekend). One-hour vehicular count was taken four times a day at 06:00–07:00 (HH:MM), 10:00–11:00 (HH:MM), 15:00–16:00 (HH:MM) and 21:00–22:00 (HH:MM). The obtained value

was averaged, and the results from vehicular count are presented in Table. S1 of supplementary text.

The collected information was subjected to statistical analysis through Statistical Package for the Social Sciences (SPSS, version: 16.0), and the level of significance was set at $p < 0.05$ for all the test performed.

### 2.3 Morphological and elemental characterization

For determining the morphology of the particles, one filter paper was randomly selected for every 15 days. Thereby, monthly, two filter papers and in total about fourteen particulate-loaded filter papers were subjected to SEM analysis. A 1 cm$^2$ portion of the filter paper was cut and coated with gold (Au) particles of thickness (15–30 nm) for 3 min using vacuum coating unit (Quorum Q150RES, Germany) for making it electrically conductive. Finally, it was analyzed with SEM (FE-SEM QUANTA 200 FEG, FEI Netherlands) available at the Institute Instrumentation Centre, IIT, Roorkee. The positioning of samples and imaging were controlled by a computer system [20].

For SEM–EDX examination, we have analyzed those particle types that are frequently found in the filter samples. The occurrence frequency of a particle type was determined through SEM examination of the filter paper. Therefore, a representative particle from each type was tested for elemental composition through SEM–EDX analysis. For this analysis, the filter papers were coated with carbon particles and subjected to a computer controlled field emission SEM–EDX (SEM laboratory, IIT New Delhi) equipped with RONTEC's EDX system Model quanTax200 (resolution: 2.0 nm @ 30 kV, accelerating voltage: 0.2–30 kV, magnification: 5× to $10^6$×). As the filter sample is coated with carbon particles, the clarity of image is usually low.

### 2.4 Satellite derived data

The spatial distribution of fire data during the study period was acquired from Moderate Resolution Imaging Spectroradiometer (MODIS) (https://firms.modaps.eosdis.nasa.gov/). The MODIS derived fire data uses one km channel at 4 and 11 μm wavelength. The shape file (*.shp*) of the fire data was acquired for graphical representation and comma-separated values file (*.csv*) was acquired for fire count data. Spatial distribution of gridded 1°×1° Aerosol Optical Depth (AOD) map was acquired from National Aeronautics and Space Administration (NASA) visualization tool called "Giovanni" (https://giovanni.gsfc.nasa.gov/giovanni). Measurement of AOD is at 550 nm from MODIS carried aboard the Terra Satellite of NASA [21].

### 2.5 Air mass back trajectory cluster analysis

To ascertain the impact of synoptic air masses on the atmospheric PM over Dehradun, 24-h air mass back trajectory converging at 500 m AGL was executed using HYbrid Single Particle Lagrangian Integrated Trajectories (HYSPLIT) [22] through Trajstat software (version 1.2.2.6) [23]. The trajectories were generated at 00:00 (HH:MM, Universal Time Coordinate). In cluster analysis, similar trajectories are averaged and the mean air mass back trajectories are visualized, thereby errors in the individual trajectories likely get balanced out. The clustering algorithm is based on Ward's hierarchical method, and Euclidean distance was selected as the cluster model. The meteorological data necessary for computing the trajectories were obtained from NCEP/NOAA global reanalysis data (ftp://arlftp.arlhq.noaa.gov/pub/archives/reanalysis). The detailed information of executing air mass back trajectories and generating cluster analysis of air mass back trajectories are discussed elsewhere [24, 25].

### 2.6 Excess cancer risk calculation

To derive the risks of inhaling the PM$_{10}$-associated metals, excess cancer risks (ECR) was calculated by many researchers using the mass concentration of carcinogenic elements such as Cr, Cd, Ni, and Pb [26, 27]. However, in the present study, ECR due to inhalation of lead (Probable human carcinogen belonging to group B2) was quantified [28]. The Inhalation Unit Risk (IUR) of Cr, Cd, and Ni can be acquired from Integrated Risk Information System (IRIS). However, human evidence of Lead is highly inadequate in IRIS; therefore, the value of IUR was obtained from California Environmental Protection Agency (Cal EPA) [29]. The IUC for Pb is 0.000012 (μg/m$^3$)$^{-1}$. The detailed methodology for calculating ECR for Lead (Pb) is mentioned elsewhere [30]. The formula for calculating the ECR is represented below

$$ECR = \frac{(C \times ET \times EF \times ED \times IUR)}{(AT)}$$

where $C$ represents concentration of the lead (μg/m$^3$), ET represents the exposure time (12 h/day), EF is the exposure frequency (184 day/year), ED is exposure duration (24 years), and AT is average time for carcinogen (AT = 24 h/day × 70 years × 365 days).

## 3 Results and discussion

### 3.1 Mass concentration of particulate matter (PM$_{10}$)

The mean ± standard deviation of PM$_{10}$ mass concentration in the winter and summer season was observed to

be $174.5 \pm 20.70$ and $142.6 \pm 36.24$ µg/m$^3$, respectively. The overall range and average of PM$_{10}$ mass concentration was observed to be 85.6–226.9 (minimum–maximum) and $158.6 \pm 33.48$ µg/m$^3$. Monthly, seasonal and weekly variation of PM$_{10}$ mass concentration is represented in Fig. 1. Independent sample student $t$ test (assuming unequal variance) revealed a significant seasonal difference in the PM$_{10}$ mass concentration during the study period ($t$-statistics $= 6.83$, $t$-critical $= 1.97$ (two-tailed), $p < 0.05$). High concentration of PM$_{10}$ in winter season can be attributed to the increased anthropogenic activities such as biomass and fossil fuel burning and meteorological parameters such as low wind speed, low planetary boundary layer and high relative humidity that can lead to a reduced rate of removal of atmospheric PM through scavenging effect [31].

The geography of the study site corresponds to a saucer-shaped valley, where dispersion of pollutants is low. Moreover, only during seven percentage of the sampling days in the entire campaign, the 24-h mean PM$_{10}$ mass concentration was less than the permissible limit of national ambient air quality standard (100 µg/m$^3$) framed by Central Pollution Control Board (CPCB), whereas none of the sampling day showed concentration less than World Health Organization's standard (50 µg/m$^3$). On comparing the results obtained in this study with other studies around the world on cities situated in a valley-based topography, it was observed that the 24-h average mass concentration of PM$_{10}$ observed at Doon valley was higher than that reported in Kathmandu valley, Nepal (127.70 µg/m$^3$) [32], Lanzhou valley, China (111.53 µg/m$^3$) [33], Piedmont region, part of Po valley, Italy (58 µg/m$^3$) [34], and Mexicalli valley, Baja California (54.5 µg/m$^3$) [35].

In the present study, approximately 28% of the sampling days were weekends (Saturday and Sunday) and 72% were weekdays (remaining days of the week). The 24-h mean PM$_{10}$ observed during weekends was $148.39 \pm 35.5$ µg/m$^3$ and during weekdays was $162.58 \pm 31.9$ µg/m$^3$. The vehicular density observed during the weekday period was 23% higher than weekends. This points toward the effect of vehicular traffic on the atmospheric PM$_{10}$ mass concentration at Dehradun.

On employing kurtosis test to the PM$_{10}$ mass concentration data, it revealed a negative value (kurtosis $= -0.72$), demonstrating a Platykurtic distribution of data (flatness of distribution of data) [36]. This distribution indicates the absence of any substantial episodic pollution event during the sampling period. Several episodic events common in India are Diwali and Holi festival. In the present study, PM$_{10}$ sampling was avoided during harsh weather conditions and festival periods.

### 3.2 Morphological characterization of atmospheric particles

Microscopic analysis reveal that the particles were mostly irregular, crystalline, smooth rounded, porous and chain-branched structures indicating various types such as tar balls, soot, biological particles, etc. (Fig. 2). Figure 2a represents tar balls. The tar balls are identified by their spherical and amorphous structures, and it usually does not aggregate with other particulates [37]. Tar balls are mostly emitted from the incomplete fossil fuel burning and biomass burning. The presence of tar balls can adversely affect the scattering and absorption of light effectively and can play an important role in climate forcing and regional haze [38].

**Fig. 1** Monthly, seasonal and weekly variation of the mean atmospheric PM$_{10}$ mass concentration along with standard deviation (bar line)
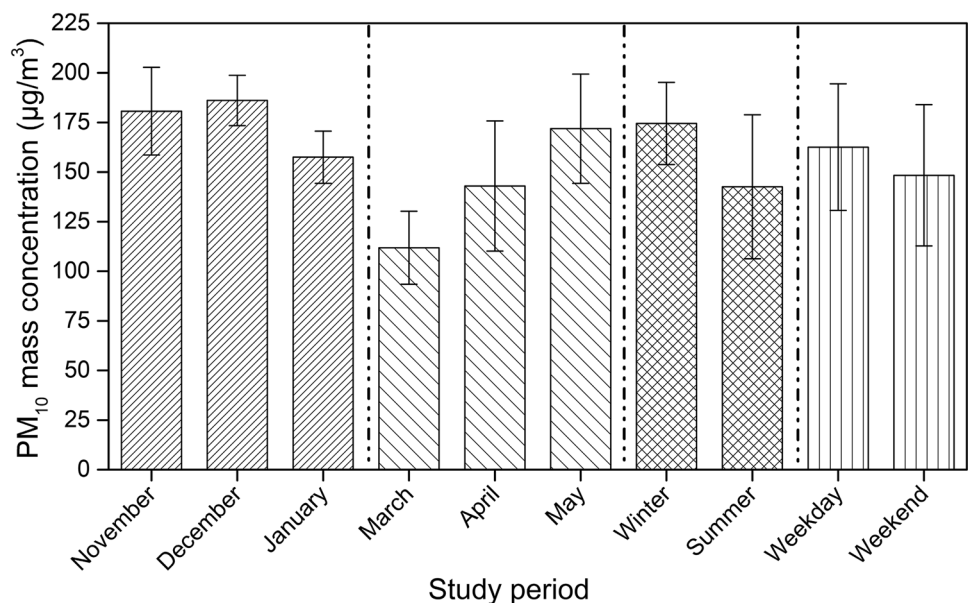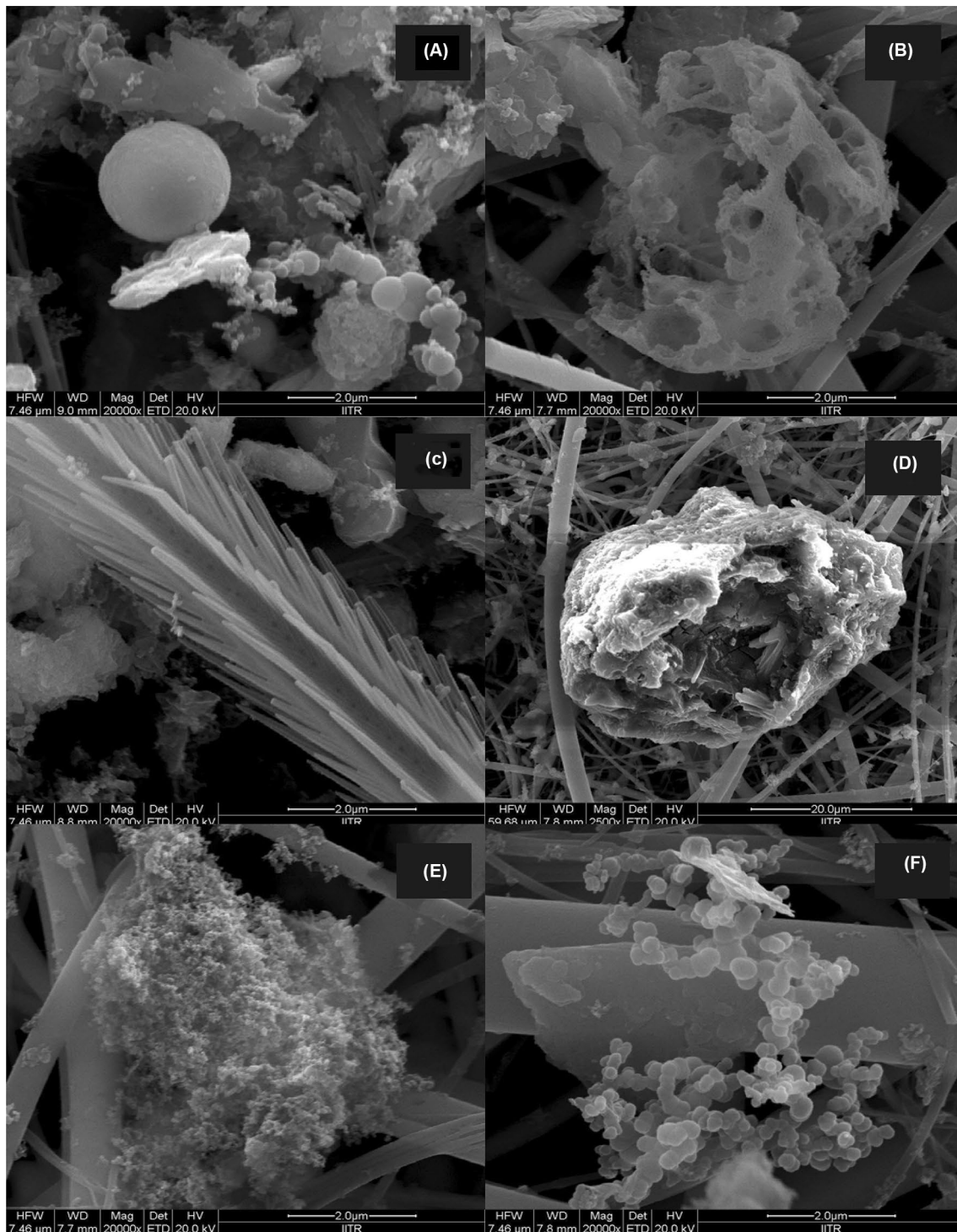
**Fig. 2** SEM image of particles: Tar balls (**a**), Porous particle (**b**), biological particle (**c**), irregular particle (**d**), soot particle (**e**), chain and branched particle (**f**)

Porous particle is represented in Fig. 2b. The origin of these particles can be attributed to the agricultural/forest burning and waste incineration. Earlier, research in morphological analysis indicates that the porous particles are rich in carbon and also has the potential to facilitate deposition of other particles leading to complex structure [9, 31].

The biological particle shown in Fig. 2c can occur due to the presence of pollens, fragments of leaves, algae, bacteria and protozoa. Also, the fragments and excrements of insects can be considered as a biological particle. Figure 2d represents an irregular particle, which can have wide variety of source and particle composition. Earlier studies in Indian region have revealed that the irregular shaped particles can be quartz, alumino-silicate, iron, chloride, and calcium-rich particles [6, 39].

Soot particles are shown in Fig. 2e, and chain/branched particles are shown in Fig. 2f. These particles are chiefly contributed from fossil fuel combustion and can be easily identified by their unique structure ranging from linear to more complex branched aggregates of particles. Their origination can also be traced to coal-burning industries and power stations involving high-temperature process [40].

### 3.3 Assessment of atomic contribution and source of trace elements through SEM–EDX

Through SEM examination, the frequently found particle types were of irregular, flaky, smooth edged and crystalline nature. A representative particle from each type was selected and analyzed for its respective chemical composition through SEM–EDX. The results from SEM–EDX analysis of four individual $PM_{10}$ particles are presented in Fig. 3 along with the respective atomic percentage contribution. The results reveal the presence of lead (Pb), cadmium (Cd), aluminum (Al), sodium (Na), calcium (Ca), iron (Fe), sulfur (S), zinc (Zn), magnesium (Mg), copper (Cu), cobalt (Co), nickel (Ni), chromium (Cr), manganese (Mn), chlorine (Cl), carbon (C) and potassium (K). The atomic percentage contribution of Si and O was high in the blank filter paper (Fig S5 of supplementary material), therefore, it was not
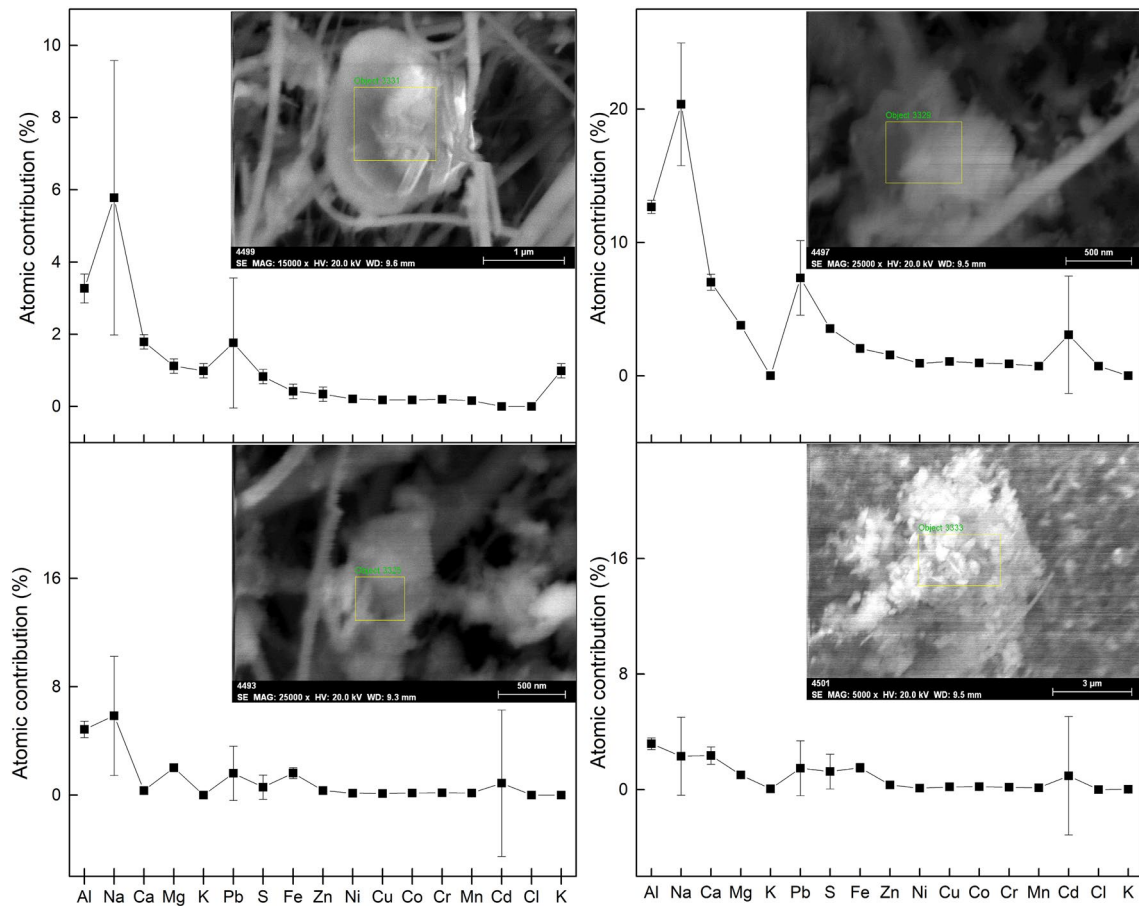


**Fig. 3** SEM–EDX results of individual particles and the respective atomic percentage contribution is represented

considered. For ease of understanding the source of these elements, the atomic percentage contribution of chemical species associated with four particles subjected to SEM–EDX test were averaged and the results are furnished in the text below.

The percentage contribution of Carbon (16.06%) was comparatively high, which can be attributed to the heavy vehicular traffic [12]. The presence of elements such as Pb (3.05%), Cr (0.36%), Zn (0.64%), Cu (0.39%) and Fe (1.41%) can be attributed to vehicular exhaust emission. The Cd (1.23%), Co (0.38%), Mn (0.30%), Ni (0.35%), and Al (6.00%) can be from the brake and tire wear [12, 41], while the presence of Na (8.58%), Ca (2.88%), Mg (1.99%), and Cl (0.19%) can be attributed to road dust re-suspension [12, 39, 42]. Further, high contribution of Pb (3.05%) in the samples can be attributed to high vehicular movement. The local sources of Pb can be attributed to the tire wear, burning of electronic and plastic waste [43, 44]. The leaded petrol which was banned from usage before a decade,

however, can exist along with the road dust for a long time [45], the road dust particles get re-suspended due to frequent movement of vehicles. Moreover, in an earlier study, elevated concentration of Pb was reported near a cement plant in the state of Chhattisgarh, India [46].

Long-range source of pollutants over Doon valley can be established owing to the presence of Sulfur (1.55%). Sulfur is chiefly emitted from coal-based thermal power plants [13]. The location of coal-based thermal power plants situated along the vicinity of sampling site was acquired and presented in Fig. 4. In addition, the air mass pathway trajectories were merged with the respective figure to investigate whether the air masses converging over Dehradun passes through these potential source regions. Detailed discussion on this portion is mentioned in Sect. 3.5.

The presence of aluminum (6.00%) can be attributed to the industrial activities like manufacturing of Al vessels, pipes and connectors, and emissions from industries in
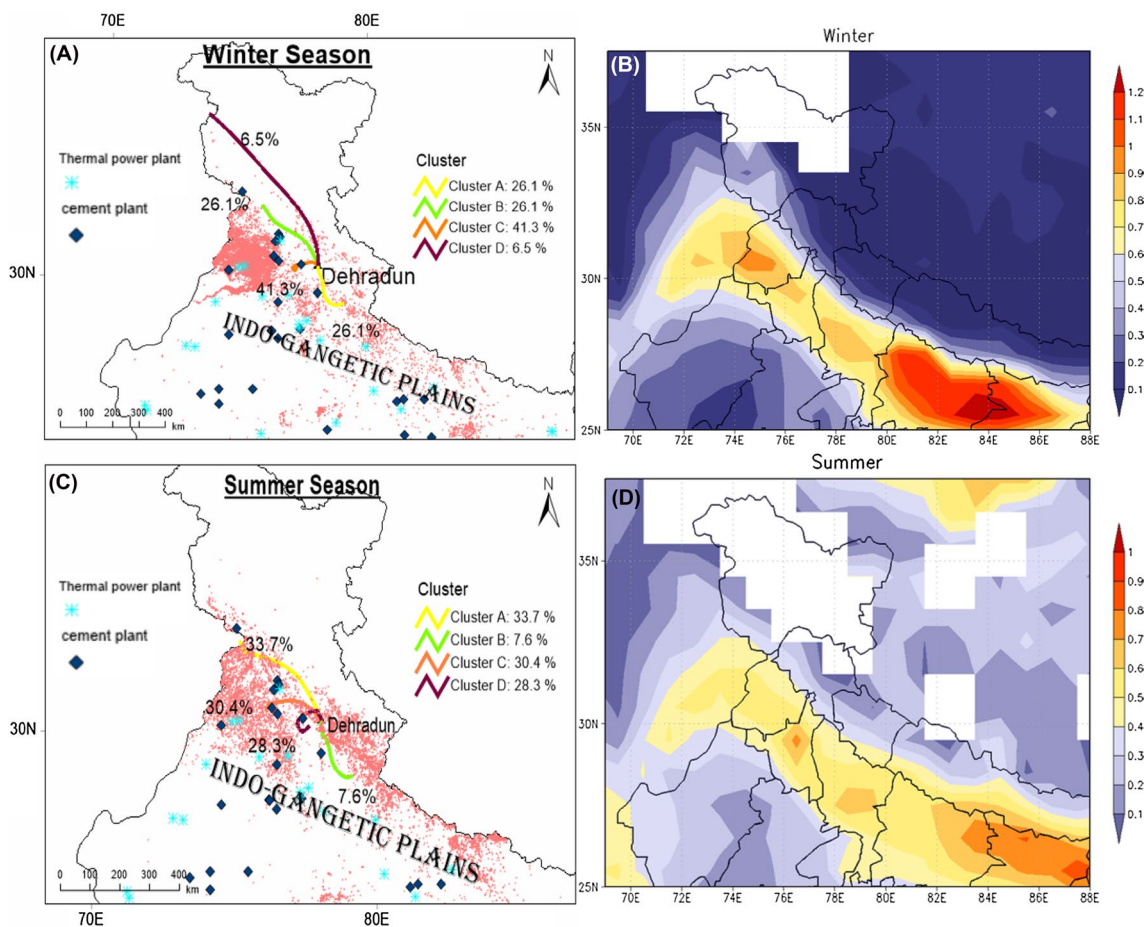


**Fig. 4** Air mass back trajectory-clusters (**a**, **b**, **c** and **d**), MODIS derived forest spots (denoted by red dots), cement industries (denoted by diamond), and thermal power plant (denoted by cross mark) around the vicinity of the sampling site during winter and summer season is represented in the left top and bottom panel, respectively. Spatial distribution of monthly average Terra-MODIS retrieved AOD (1°×1°) at 550 nm is represented in the right top (winter season) and bottom figures (summer season)

the form of fly ash [20]. The complex structure observed in Fig. 2e may have been triggered by high-temperature combustion processes, which is common in manufacturing industries. These results suggest that the air quality over Dehradun can be substantially influenced by the anthropogenic activities such as industrial and vehicular movement.

### 3.4 Excess cancer risks due to inhalation of $PM_{10}$ laden Lead (Pb)

Among the anthropogenic originated elements, high atomic contribution of Pb (3.05%) prompted us to quantify the mass concentration of Pb in $PM_{10}$ samples. The Pb was quantified by subjecting the particulate-loaded filter paper to Atomic Absorption Spectroscopy (AAS). One filter paper per week was selected for the analysis, therefore in total, about twenty-seven filter papers were subjected to AAS analysis. The methodology used for quantification was according to Shridhar et al. [47]. The step-wise protocol followed for the analysis and obtained results are described in brief in the supplementary text. The mean concentration of Pb associated with the atmospheric $PM_{10}$ samples collected during the study period was observed to be 0.159 μg/$m^3$ (Fig. S6 of the supplementary text). Therefore, the ECR due to inhalation of atmospheric Pb was observed to be $0.16 \times 10^{-6}$, which is well below the safe limit of $1 \times 10^{-6}$. For public health protection, the United States Environment Protection Agency has recommended the safe limit of ECR value to be one in a million ($1 \times 10^{-6}$) [48].

### 3.5 Influence of biomass/fuel wood burning on air quality

Impact of biomass burning/forest fire on the air quality of Dehradun can be substantiated by the presence of K in all the four particle types. The presence of K (0.26%) in all the analyzed particles tempted us to acquire MODIS derived fire data and aerosol optical depth around the vicinity of the sampling site, as it is well known that the presence of K in the atmospheric PM denotes substantial contribution from biomass burning [2, 49]. Figure 4 reveals high fire counts around the sampling site, which points to the extent of how biomass burning emissions can influence the air quality of Dehradun city. Moreover, in India, the monthly fire counts reported during the study period followed the order of April (5214) > March (5174) > May (1260) > November (1143) > January (474) > December (284); month (fire counts). High fire counts during summer season is due to crop-residue burning in IGP and forest fire in the Himalayan region [50], while fire counts during November is chiefly attributed to the crop-residue burning

in the north-western IGP [21]. The pollutants released from these locations can travel to far end places through long-range transport. In a comprehensive study, Rupakheti et al. [51] reported that open fire in IGP region during pre-monsoon period lead to a surge in pollution level at Lumbini, a famous tourist site located near the northern edge of central-IGP. However, in this study, we are reporting the influence of emissions from IGP and Himalayan region over Dehradun city, which is located near the foothills of the Himalayas.

In support of the earlier results, the spatial distribution of aerosol optical depth (AOD) derived from MODIS-Terra satellite reveal seasonal difference. During winter season, there is an increase in the biomass burning over IGP region and so higher AOD was observed (Fig. 4). Likewise, during summer season, the mountainous region in Uttarakhand shows an elevated AOD which can be chiefly attributed to the forest fire [50]. Previous studies indicate that emissions from forest/biomass burning are one of the chief sources of soot and tar balls in the atmosphere [38].

Furthermore, earlier research shows that people in the state of Uttarakhand depend mostly on the fuelwood for cooking, so the region has higher consumption of fuel wood (average: 1.50–2.50 kg per capita per day) compared to the central Himalayan region (1.49 kg per capita per day) [52–54]. Therefore, apart from forest fire burning emissions, fuelwood can also influence the air quality in the surrounding region. An earlier study revealed that the PM estimate from biomass fuel is about 8.61 ± 4.54 Gg/year, which is higher than several north Indian states [55].

### 3.6 Cluster analysis of backward air mass trajectory

In the earlier section, the biomass burning, cement and coal-based thermal power plant emissions were presumed to play a substantial role in influencing the air quality of Dehradun. However, it is recommended to have a detailed knowledge of the pathways traversed by the air masses converging over Dehradun. Therefore, air mass back trajectory analysis was performed to investigate whether the air masses converging over Dehradun city is influenced by forest fire/biomass burning, emission from the coal-based thermal power plant and/or from cement industries in the vicinity (Fig. 4).

Trajectory cluster analysis indicates that the air masses have its source mostly from north-western direction from Dehradun city. To represent the predominant direction of air masses, four number of clusters (A, B, C and D) were generated from the 24-h air mass back trajectories for winter and summer season. In the course of winter season, clusters B and D represent 26.1 and 6.5% of the trajectories each; these trajectories had long-range sources from

the northern part of India. Cluster A and C representing 26.1 and 41.3% of the trajectories originate from the Indo-Gangetic Plains (IGP), where high fire counts was observed. Also, IGP has high number of cement and coal-based thermal power plants. Therefore, it can be mentioned that the air masses from cluster B and C can have greater influence on the air quality over Dehradun.

In the summer season, trajectories were mostly from north-western direction from the receptor site. Cluster A and C sharing around 33.7 and 30.4% of the trajectories originated from north-western IGP, where large quantity of agricultural/residue burning are reported. Moreover, earlier studies have reported that these regions are dotted with many industrial hubs [56] and hundreds of brick kilns located in these regions release higher quantity of emission due to poor technology used in the manufacturing processes [57]. Cluster B and D representing 7.6 and 28.3% of trajectories originate from central-IGP.

## 4 Conclusions

1. The findings of this study indicate that during 93% of sampling days, the $PM_{10}$ mass concentration was more than the permissible limit of Central Pollution Control Board (100 μg/m³) and during all days of sampling, the atmospheric $PM_{10}$ level was higher than the permissible limit of WHO (50 μg/m³)

2. Microscopic analysis reveal that the morphology of particles were mostly irregular, smooth rounded, flaky, porous and chain-branched structures indicating various types such as tar balls, soot, crystalline, biological particles, etc.

3. SEM–EDX result indicates that the atomic contribution of anthropogenic (Pb, Cr, Cd, Cu, Co, Zn, Mn, and Ni) and crustal/soil (Na, Ca, Cl, Al, Mg, Fe, and K) elements were 22.1 and 77.8%, respectively. This indicates that the road dust re-suspension, vehicular exhaust, and industrial emission play a considerable role in air quality degradation over the city.

4. Trajectory cluster analysis reveal that the source and transport pathway of air masses were mostly through the IGP and Indo-Himalayan region. The forest fire and aerosol optical depth maps indicate that the IGP region has high frequency of biomass burning activities during November, while Himalayan region has high frequency of forest fire during April and May. The emissions from these burning activities influence the air quality at Dehradun. Moreover, it is possible that Dehradun may be influenced by emissions from the coal-based thermal power plants and cement industries situated in its vicinity, as the air masses converg-

ing over Doon valley traverse across locations where several industrial hubs are situated.

5. The excess cancer risks due to inhalation of atmospheric Pb associated with $PM_{10}$ was observed to be $0.16 \times 10^{-6}$.

The results from this pioneering study will be helpful in understanding the aerosol dynamics over an urban valley like Dehradun. In future, sampling of atmospheric particles can be carried out using non-fiber based filter material so that in-depth morphological analysis through image processing software is possible.

## Compliance with the ethical standards

**Conflict of interest** The authors declare that they have no conflict of interest.

## References

1. USEPA (2015) Criteria air pollutants. Am Child Environ 1–22. http://www.epa.gov/criteria-air-pollutants
2. Banerjee T, Murari V, Kumar M, Raju MP (2015) Source apportionment of airborne particulates through receptor modelling: Indian scenario. Atmos Res 164–165:167–187. https://doi.org/10.1016/j.atmosres.2015.04.017
3. Samiksha S, Raman RS, Nirmalkar J, Kumar S, Sirvaiya R (2017) $PM_{10}$ and $PM_{2.5}$ chemical source profiles with optical attenuation and health risk indicators of paved and unpaved road dust in Bhopal, India. Environ Pollut. https://doi.org/10.1016/j.envpol.2016.11.067
4. Bhuyan P, Deka P, Prakash A, Balachandran S, Hoque RR (2018) Chemical characterization and source apportionment of aerosol over mid Brahmaputra Valley, India. Environ Pollut 234(2018):997–1010. https://doi.org/10.1016/j.envpol.2017.12.009
5. Gupta S, Gadi R, Sharma SK, Mandal TK (2018) Characterization and source apportionment of organic compounds in PM10 using PCA and PMF at a traffic hotspot of Delhi. Sustain Cities Soc 39:52–67. https://doi.org/10.1016/j.scs.2018.01.051
6. Pachauri T, Singla V, Satsangi A, Lakhani A, Kumari MK (2013) SEM–EDX characterization of individual coarse particles in Agra, India. Aerosol Air Qual Res 13:523–536. https://doi.org/10.4209/aaqr.2012.04.0095
7. Margiotta S, Lettino A, Speranza A, Summa V (2015) $PM_1$ geochemical and mineralogical characterization using SEM-EDX to identify particle origin—Agri Valley pilot area (Basilicata, southern Italy). Nat Hazards Earth Syst Sci 15:1551–1561. https://doi.org/10.5194/nhess-15-1551-2015
8. Ault AP, Peters TM, Sawvel EJ, Casuccio GS, Willis RD, Norris GA, Grassian VH (2012) Single-particle SEM–EDX analysis of iron-containing coarse particulate matter in an urban environment: sources and distribution of iron within Cleveland, Ohio. Environ Sci Technol 46:4331–4339. https://doi.org/10.1021/es204006k

9. Nagendra SMS, Diya M, Chithra VS, Menon JS, Peter AE (2016) Characteristics of air pollutants at near and far field regions of a national highway located at an industrial complex. Transp Res Part D Transp Environ 48:1–13. https://doi.org/10.1016/j.trd.2016.07.006

10. Chithra VS, Nagendra SMS (2013) Chemical and morphological characteristics of indoor and outdoor particulate matter in an urban environment. Atmos Environ 77:579–587. https://doi.org/10.1016/j.atmosenv.2013.05.044

11. Pipal AS, Kulshrestha A, Taneja A (2011) Characterization and morphological analysis of airborne PM2.5 and PM10 in Agra located in north central India. Atmos Environ 45:3621–3630. https://doi.org/10.1016/j.atmosenv.2011.03.062

12. Srivastava A, Jain VK, Srivastava A (2009) SEM-EDX analysis of various sizes aerosols in Delhi India. Environ Monit Assess. https://doi.org/10.1007/s10661-008-0239-0

13. Srivastava D, Goel A, Agrawal M (2016) Particle bound metals at major intersections in an urban location and source identification through use of metal markers. Proc Natl Acad Sci India Sect A Phys Sci 86(2):209–220. https://doi.org/10.1007/s40010-016-0268-y

14. Singh N, Murari V, Kumar M, Barman SC, Banerjee T (2017) Fine particulates over South Asia: review and meta-analysis of PM$_{2.5}$ source apportionment through receptor model. Environ Pollut 223:121–136. https://doi.org/10.1016/j.envpol.2016.12.071

15. Correia A, Pope CA, Dockery DW, Wang Y, Ezzati M, Dominici F (2013) The effect of air pollution control on life expectancy in the United States: an analysis of 545 US counties for the period 2000–2007. Epidemiology 24:23–31. https://doi.org/10.1097/EDE.0b013e3182770237

16. Izhar S, Goel A, Chakraborty A, Gupta T (2016) Annual trends in occurrence of submicron particles in ambient air and health risk posed by particle bound metals. Chemosphere 146:582–590. https://doi.org/10.1016/j.chemosphere.2015.12.039

17. Dutta D, Rahman A, Kundu A (2015) Growth of Dehradun city: an application of linear spectral unmixing (LSU) technique using multi-temporal landsat satellite data sets. Remote Sens Appl Soc Environ 1:98–111. https://doi.org/10.1016/j.rsase.2015.07.001

18. WHO (2016) Ambient air pollution 2016. http://www.who.int/phe/health_topics/outdoorair/databases/cities/en/. Accessed 9 Nov 2018

19. Prabhu V, Gupta SK, Madhwal S, Shridhar V (2019) Exposure to atmospheric particulates and associated respirable deposition dose to street vendors at residential and commercial site in Dehradun city. Saf Health Work. https://doi.org/10.1016/j.shaw.2019.01.005

20. Murari V, Kumar M, Singh N, Singh RS, Banerjee T (2015) Particulate morphology and elemental characteristics: variability at middle Indo-Gangetic Plain. J Atmos Chem 73:165–179. https://doi.org/10.1007/s10874-015-9321-5

21. Badarinath KVS, Kharol SK, Sharma AR (2009) Long-range transport of aerosols from agriculture crop residue burning in Indo-Gangetic Plains–a study using LIDAR, ground measurements and satellite data. J Atmos Sol Terr Phys 71:112–120. https://doi.org/10.1016/j.jastp.2008.09.035

22. Draxler RR, Rolph GD (2003). Hybrid single-particle lagrangian integrated trajectory (HYSPLIT) model. NOAA Air Resour Lab Silver Spring, MD

23. Wang YQ, Zhang XY, Draxler RR (2009) Environmental modelling & software TrajStat: GIS-based software that uses various trajectory statistical analysis methods to identify potential sources from long-term air pollution measurement data. Environ Model Softw 24:938–939. https://doi.org/10.1016/j.envsoft.2009.01.004

24. Sen A, Abdelmaksoud AS, Ahammed YN, Alghamdi M, Banerjee T, Bhat MA, Chaterjee A, Choudhuri AK, Das T, Dhir A, Dhyani PP, Gadi R, Ghosh S, Kumar K, Khan A, Khoder M, Kumari M, Kuniyal JC, Kumar M, Lakhani A, Mahapatra PS, Naja M, Pal D, Pal S, Rafiq M, Romshoo SA, Rashid I, Saikia P, Shenoy D, Sridhar V, Verma N, Vyas B, Saxena M, Sharma A, Sharma S, Mandam T (2017) Variations in particulate matter over Indo-Gangetic Plains and Indo-Himalayan Range during four field campaigns in winter monsoon and summer monsoon: role of pollution pathways. Atmos Environ 154:200–224. https://doi.org/10.1016/j.atmosenv.2016.12.054

25. Prabhu V, Shridhar V (2019) Investigation of potential sources, transport pathway, and health risks associated with respirable suspended particulate matter in Dehradun city, situated in the foothills of the Himalayas. Atmos Pollut Res. https://doi.org/10.1016/j.apr.2018.07.009

26. Khillare PS, Sarkar S (2012) Airborne inhalable metals in residential areas of Delhi, India: distribution, source apportionment and health risks. Atmos Pollut Res 3:46–54. https://doi.org/10.5094/APR.2012.004

27. Hieu NT, Lee BK (2010) Characteristics of particulate matter and metals in the ambient air from a residential area in the largest industrial city in Korea. Atmos Res 98:526–537. https://doi.org/10.1016/j.atmosres.2010.08.019

28. IRIS (1995) United States Environmental Protection Agency. https://www.epa.gov/IRIS/. Accessed 11 Dec 2018

29. Khanna I, Khare M, Gargava P (2015) Health risks associated with heavy metals in fine particulate matter: a case study in Delhi City, India. J Geosci Environ Prot 3:72–77. https://doi.org/10.4236/gep.2015.32012

30. Prakash J, Lohia T, Mandariya AK, Habib G, Gupta T, Gupta SK (2018) Chemical characterization and quantitativ e assessment of source-specific health risk of trace metals in PM1.0 at a road site of Delhi, India. Environ Sci Pollut Res 25:8747–8764. https://doi.org/10.1007/s11356-017-1174-9

31. Panda S, Nagendra SMS (2018) Chemical and morphological characterization of respirable suspended particulate matter (PM$_{10}$) and associated heath risk at a critically polluted industrial cluster. Atmos Pollut Res. https://doi.org/10.1016/j.apr.2018.01.011

32. Kim BM, Park JS, Kim SW, Kim H, Jeon H, Cho C, Kim JH, Hong S, Rupakheti M, Panday AK, Park RJ, Hong J, Yoon SC (2015) Source apportionment of PM$_{10}$ mass and particulate carbon in the Kathmandu Valley, Nepal. Atmos Environ 123:190–199. https://doi.org/10.1016/j.atmosenv.2015.10.082

33. Xiao Z, Shao L, Zhang N, Wang J, Wang J (2013) Heavy metal compositions and bioreactivity of airborne PM$_{10}$ in a Valley-Shaped City in Northwestern China. Aerosol Air Qual Res 13:1116–1125. https://doi.org/10.4209/aaqr.2012.10.0287

34. Padoan E, Malandrino M, Giacomino A, Grosa MM, Lollobrigida F, Martini S, Abollino O (2016) Spatial distribution and potential sources of trace elements in PM$_{10}$ monitored in urban and rural sites of Piedmont Region. Chemosphere 145:495–507. https://doi.org/10.1016/j.chemosphere.2015.11.094

35. Canales-Rodríguez M, Quintero-Núñez M, Valdés-Salas B, Daessle-Heuser W (2015) Distribution and characterization of PM$_{10}$ in City and Valley of Mexicali, Baja California, Mexico. J Environ Prot (Irvine, Calif) 06:25–33. https://doi.org/10.4236/jep.2015.61004

36. Salkind N (2010) Encyclopedia of research design, vol 1. SAGE, Thousand Oaks

37. Cong Z, Kang S, Dong S, Liu X, Qin D (2010) Elemental and individual particle analysis of atmospheric aerosols from high Himalayas. Environ Monit Assess. https://doi.org/10.1007/s10661-008-0698-3

38. Hand JL, Malm WC, Laskin A, Day D, Lee T, Wang C, Carrico C, Carrillo J, Cowin JP, Collett J, Iedema J (2005) Optical, physical, and chemical properties of tar balls observed during the Yosemite Aerosol Characterization Study. J Geophys Res Atmos 110:1–14. https://doi.org/10.1029/2004JD005728

39. Pipal AS, Kulshrestha A, Taneja A (2011) Characterization and morphological analysis of airborne $PM_{2.5}$ and $PM_{10}$ in Agra located in north central India. Atmos Environ 45:3621–3630. https://doi.org/10.1016/j.atmosenv.2011.03.062

40. Gao Y, Ji H (2018) Microscopic morphology and seasonal variation of health effect arising from heavy metals in $PM_{2.5}$ and $PM_{10}$: 1-year measurement in a densely populated area of urban Beijing. Atmos Res 212:213–226. https://doi.org/10.1016/j.atmosres.2018.04.027

41. Srimuruganandam B, Nagendra SMS (2012) Source characterization of $PM_{10}$ and $PM_{2.5}$ mass using a chemical mass balance model at urban roadside. Sci Total Environ 433:8–19. https://doi.org/10.1016/j.scitotenv.2012.05.082

42. Begum BA, Biswas SK, Hopke PK (2011) Key issues in controlling air pollutants in Dhaka, Bangladesh. Atmos Environ 45:7705–7713. https://doi.org/10.1016/j.atmosenv.2010.10.022

43. Spada N, Bozlaker A, Chellam S (2012) Multi-elemental characterization of tunnel and road dusts in Houston, Texas using dynamic reaction cell-quadrupole-inductively coupled plasma-mass spectrometry: evidence for the release of platinum group and anthropogenic metals from motor vehicles. Anal Chim Acta 735:1–8. https://doi.org/10.1016/j.aca.2012.05.026

44. Pant P, Baker SJ, Shukla A, Maikawa C, Godri KJ, Harrison RM (2015) The PM10 fraction of road dust in the UK and India: characterization, source profiles and oxidative potential. Sci Total Environ 530–531:445–452. https://doi.org/10.1016/j.scitotenv.2015.05.084

45. Sen IS, Bizimis M, Tripathi SN, Paul D (2016) Lead isotopic fingerprinting of aerosols to characterize the sources of atmospheric lead in an industrial city of India. Atmos Environ 129:27–33

46. Sharma R, Pervez S (2004) Chemical characterization and enrichment of selected toxic elements in ambient particulate matter around a slag based cement plant in Chhattisgarh state—a case study. J Sci Ind Res (India) 63:376–382

47. Shridhar V, Khillare PS, Agarwal T, Ray S (2010) Metallic species in ambient particulate matter at rural and urban location of Delhi. J Hazard Mater 175:600–607. https://doi.org/10.1016/j.jhazmat.2009.10.047

48. USEPA (2009) Risk assessment guidance for superfund (RAGS), Volume 1 human health evaluation manual (Part F, Supplemental guidance for inhalation risk assessment), EPA-540-R-070-002

49. Pachon JE, Weber RJ, Zhang X, Mulholland JA, Russell AG (2013) Revising the use of potassium (K) in the source apportionment of $PM_{2.5}$. Atmos Pollut Res 4:14–21. https://doi.org/10.5094/APR.2013.002

50. Giglio L, Csiszar I, Justice CO (2006) Global distribution and seasonality of active fires as observed with the terra and aqua moderate resolution imaging spectroradiometer (MODIS) sensors. J Geophys Res Biogeosci 111:1–12. https://doi.org/10.1029/2005JG000142

51. Rupakheti D, Adhikary B, Praveen PS, Rupakheti M, Kang S, Mahata KS, Naja M, Zhang Q, Panday AK, Lawrence MG (2017) Pre-monsoon air quality over Lumbini, a world heritage site along the Himalayan foothills. Atmos Chem Phys 17:11041–11063. https://doi.org/10.5194/acp-17-11041-2017

52. Chettri N, Sharma E, Deb DC, Sundriyal RC (2006) Impact of firewood extraction on tree structure, regeneration and woody biomass productivity in a trekking corridor of the Sikkim Himalaya. Mt Res Dev 22:150–158. https://doi.org/10.1659/0276-4741(2002)022%5b0150:iofeot%5d2.0.co;2

53. Sati VP (2008) Natural resource conditions and economic development in the Uttaranchal Himalaya, India. J Mt Sci 2:336–350. https://doi.org/10.1007/bf02918407

54. Kumar M, Sharma CM (2009) Fuelwood consumption pattern at different altitudes in rural areas of Garhwal Himalaya. Biomass Bioenergy 33:1413–1418. https://doi.org/10.1016/j.biombioe.2009.06.003

55. Saxena M, Sharma SK, Tomar N, Ghayas H, Sen A, Garhwal RS, Gupta NC, Mandal TK (2016) Residential biomass burning emissions over Northwestern Himalayan region of India: chemical characterization and budget estimation. Aerosol Air Qual Res 16:504–518. https://doi.org/10.4209/aaqr.2015.04.0237

56. Singh AL, Asgher MS (2005) Impact of brick kilns on land use/landcover changes around Aligarh city, India. Habitat Int 29:591–602. https://doi.org/10.1016/j.habitatint.2004.04.010

57. Rajarathnam U, Athalye V, Ragavan S, Maithel S, Lalchandani D, Kumar S, Baum E, Weyant C, Bond T (2014) Assessment of air pollutant emissions from brick kilns. Atmos Environ 98:549–553. https://doi.org/10.1016/j.atmosenv.2014.08.075